Bioorganic Chemistry 83 (2019) 235–241

Contents lists available at ScienceDirect

Bioorganic Chemistry

journal homepage: www.elsevier.com/locate/bioorg

Carbazole and hydrazone derivatives as new competitive inhibitors of tyrosinase: Experimental clues to binuclear copper active site binding

Usman Ghani

Clinical Biochemistry Unit, Department of Pathology, College of Medicine, King Saud University, Riyadh 11461, Saudi Arabia

ARTICLE INFO

Keywords:
Tyrosinase
Carbazole
Hydrazone
Inhibitor
Competitive
Kinetics
Binuclear copper center

ABSTRACT

In this work a total of 12 carbazoles and hydrazone-bridged thiazole-pyrrole derivatives have been identified as new competitive inhibitors of tyrosinase. Carbazole derivative with 2-benzoimidazole substitution showed most potent inhibition in the series. Other carbazole derivatives containing benzothiazole and benzoxazole substitutions showed comparable levels of tyrosinase inhibition. The hydrazone derivatives also showed potent tyrosinase inhibitory activity with comparable K_i values except one with fluoride at its terminal position. Kinetic studies showed competitive inhibition of tyrosinase by all compounds that increased the substrate K_m without changing the V_{max} value. Moreover, experimental evidence suggests that the target compounds specifically bind to the binuclear copper center of the tyrosinase active site in an apparent mono-dentate fashion. Carbazoles and hydrazones are new and emerging classes of compounds as tyrosinase inhibitors that may provide new structural avenues to discovery of drugs targeting the treatment of hyperpigmentation and related dermatological disorders.

1. Introduction

Melanogenesis in the skin, eyes and hair is a natural and protective process in humans, mammals and other animals in which tyrosinase plays a pivotal role in melanin synthesis. The enzyme participates in both monophenolase and *o*-diphenolase activities by catalyzing the hydroxylation and oxidation of monophenols to *o*-quinones and oxidation of *o*-diphenols to *o*-quinones in the Raper-Mason pathway of melanogenesis [1]. Inhibition of tyrosinase is an important clinical target in dermatology for treating skin disorders such as melasma, post-inflammatory melanoderma, flecks, lentigo, nevus, ephelis and melanoma of pregnancy [2–6]. Tyrosinase inhibitors are becoming important therapeutic agents in a number of prescription drugs and cosmetic products used for the treatment of skin hyperpigmentation manifested in various clinical conditions and for skin-lightening effects for cosmetic purposes. The most common example is kojic acid, a potent tyrosinase inhibitor that has been clinically used in topical preparations to treat post-inflammatory hyperpigmentation and associated conditions in addition to its use in creams and lotions for cosmetic effects [7]. Tyrosinase inhibition is also a target for preventing undesirable fruit browning and extending its shelf-life for potential commercial and economical benefits [8]. Moreover, molting and wound-healing processes in insects deploy tyrosinase for melanin generation, and inhibition of the enzyme provides potential targets for developing safer and effective insecticides for insect control [9].

Carbazole and its derivatives are nitrogen containing aromatic heterocyclic compounds with diverse biological effects including antimicrobial, anti-tumor, anti-inflammatory, anti-oxidative and anti-histamine activities. Derivatives of triazoles, imidazoles and benzimidazoles are well known antimicrobial agents used for the treatment of a variety of fungal and bacterial infections [10]. The carbazole moiety is also distributed in many active natural products including carbazomycins that are antibiotics [11,12]. Thiazole and its derivatives are a well-known group of compounds with anti-hypertensive, anti-allergic, anti-inflammatory, anti-schizophrenic and anti-HIV activities. Thiazole-hydrazone conjugates are particularly known for their anti-microbial activity [13]. Furthermore, a number of azole ring-containing compounds are also known to potently inhibit tyrosinase. Examples include various thidiazole, oxadiazole and triazole derivatives [14–21]. Carbazole and hydrazone derivatives are new and emerging classes of compounds with tyrosinase inhibitory activity. Carbazole-substituted chalcone urea derivatives have been previously reported to inhibit *o*-diphenolase activity of banana tyrosinase [22].

The current work reports seven carbazoles and five hydrazone-bridged thiazole-pyrrole derivatives (henceforth hydrazone derivatives) as new competitive inhibitors of tyrosinase synthesized previously. Experimental evidence revealed that the target compounds bind to the tyrosinase active site by interacting with its binuclear copper center.

E-mail addresses: ughani@ksu.edu.sa, ughani@gmx.net.

https://doi.org/10.1016/j.bioorg.2018.10.026
Received 8 April 2018; Received in revised form 11 October 2018; Accepted 15 October 2018
Available online 19 October 2018

The compounds are proposed to interact with the binuclear center in a mono-dentate manner supporting the rationale based on the X-ray crystallographic structures of the mushroom tyrosinase and catechol oxidase active sites [23,24]. To date, this is the first report on the competitive inhibition of tyrosinase by carbazole and hydrazone-bridged thiazole-pyrrole derivatives and their proposed active site binding mode that may provide new approaches to discovery of tyrosinase inhibitors for the treatment of hyperpigmentation and other dermatological disorders.

2. Materials and methods

2.1. Synthesis of carbazole and hydrazone derivatives

The design, synthesis and all physical and chemical analyses of the carbazole (**CB1–CB7**) [10,25] and hydrazone derivatives (**HZ1–HZ5**) [13] have been previously conducted and reported elsewhere.

2.2. Tyrosinase inhibition assay

Tyrosinase inhibition assay was designed and modified using the method reported elsewhere [26]. The 300 µl reaction mixture contained 50 mM sodium phosphate buffer (pH 6.8), 850 U mushroom tyrosinase (EC 1.14.18.1) (Sigma Chemical Co., St. Louis, USA), 1.0 mM L-DOPA and the target compounds dissolved in DMSO. The final concentration of DMSO in the reaction mixture was 3%. The *o*-diphenolase inhibitory activity of the compounds was tested in 96-well microplates in a SpectraMax Plus 384® microplate reader (Molecular Devices, California, USA). The compounds were initially pre-incubated with the enzyme for 15 min. at 25 °C, and the production of dopachrome was continuously monitored at 475 nm. for 2 min. at 25 °C. The *o*-diphenolase inhibitory activity of the compounds was compared with that of kojic acid as a positive control.

2.3. Tyrosinase inhibition kinetics

The experimental protocol followed for tyrosinase inhibition kinetics was the same as mentioned above except that the reaction mixture contained a range of L-DOPA (0.25–2.0 mM) and inhibitor concentrations. The initial enzyme velocities, in the absence and presence of inhibitors, were calculated from the linear portion of each curve. The K_i values of the inhibitors were calculated from Dixon plot and the type of inhibition was confirmed by Lineweaver-Burke plot using Grafit 7.0.3 (Erithacus Software Ltd., Staines, UK). Mean K_i and values and their standard error of mean (SEM) were determined from each of four individual experiments.

2.4. Binuclear copper binding assay

The binuclear copper binding assay was adapted from the method described elsewhere [27]. Tyrosinase was maximally inhibited by incubating it with the highest concentration of the target compounds followed by addition of a range of $CuSO_4$ concentrations (0.01–0.65 mM). The reaction was monitored at 475 nm in 96-well microplates in a SpectraMax Plus 384® microplate reader. The recovery of the pre-inhibited tyrosinase activity was indicated by an increase in absorbance after addition of $CuSO_4$. The effect of $CuSO_4$ on tyrosinase alone was also determined by incubating the enzyme with a range of $CuSO_4$ concentrations (0.04–0.36 mM) and measuring the remaining enzyme activity.

3. Results and discussion

3.1. Inhibition of o-diphenolase activity of tyrosinase

The target compounds exhibited concentration-dependent

Table 1
The structures and K_i values of the carbazole and hydrazone tyrosinase inhibitors.

No.	R	K_i (µM ± SEM)
	Carbazole inhibitors	
CB1	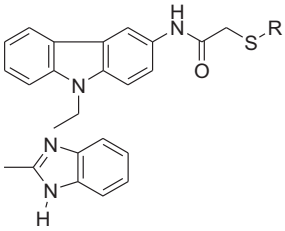	1.64 ± 0.03
CB2	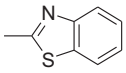	6.87 ± 0.17
CB3	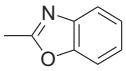	4.34 ± 0.04
CB4		3.46 ± 0.07
CB5	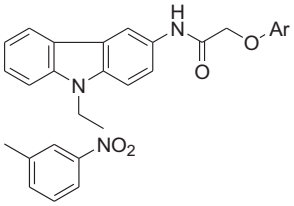	5.41 ± 0.15
CB6	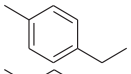	6.73 ± 0.21
CB7	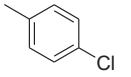	7.48 ± 0.19
	Hydrazone inhibitors	
HZ1	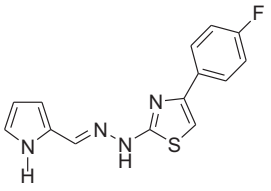	21.45 ± 0.80
HZ2	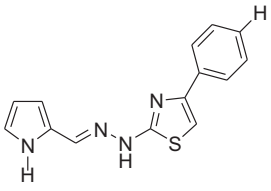	5.81 ± 0.16
HZ3	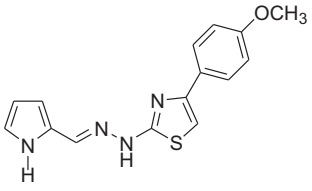	5.94 ± 0.22
HZ4	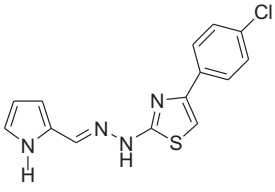	4.95 ± 0.19

(*continued on next page*)

Table 1 (*continued*)

No.	R	K_i (μM ± SEM)
HZ5	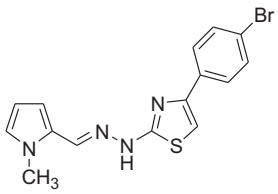	6.06 ± 0.27
Kojic acid		4.43 ± 0.20

inhibition of *o*-diphenolase activity of mushroom tyrosinase as indicated by their ability to decrease final absorbance when compared to respective controls containing no inhibitors. The K_i values of majority of the compounds were comparable to that of kojic acid – a standard inhibitor of tyrosinase (Table 1). Some derivatives such as **CB1**, **CB3** and **CB4** were found to be more potent than kojic acid. Moreover, some members of the carbazole series (K_i range = 1.64–7.48 μM) were more potent than that of hydrazones. The K_i values of the hydrazone derivatives ranged from 4.95 to 21.45 μM possessing comparable potency of inhibition with that of kojic acid.

3.2. Kinetic studies

A significant decrease in the enzyme reaction rates was observed in the presence of the target compounds when compared to their respective controls containing no inhibitor. An increasing order of inhibition potency i.e. carbazoles > hydrazones was observed. The activity of the compounds depended on the class of the parent structure including the type and position of various substitutions.

The initial raw data were screened for best fit using the Lineweaver-Burk plot [28] with the Michaelis-Menten equation transformed to various types of inhibition with least standard error. All compounds exhibited competitive inhibition of mushroom tyrosinase as determined and confirmed by the Lineweaver-Burk plot {$1/v$ versus $1/[S]$}. The plots yielded all lines converging at the same point on the *y*-axis with variable *x*-intercepts, typical of competitive inhibition. The K_i values were calculated using the Dixon plot {$1/v$ versus [I]} [29]. The values of V_{max} and K_m, following the inhibition of mushroom tyrosinase by the compounds, were in agreement with competitive inhibition that is characterized by an increase in the substrate K_m with no change in the V_{max} value (Fig. 1). The Lineweaver-Burk and their corresponding Dixon plots for representative compounds from each of the carbazole and hydrazone series are presented in Fig. 2 and Fig. 3 respectively. The structures and K_i values for the carbazole and hydrazone derivatives are listed in Table 1.

3.3. Binuclear copper–inhibitor binding

The rationale for binuclear copper center binding of the target compounds is centered on the experimental and structural evidence from the crystal structures of mushroom tyrosinase in complex with tropolone [23] and catechol oxidase in complex with phenylthiourea (PTU) [24]. The active sites of both of the enzymes share significant homology in terms of active site structure and catalysis.

The crystal structure of mushroom tyrosinase in complex with tropolone reveals that its H subunit contains the binuclear copper-binding site at the center of four α-helices that is located at the bottom of a large cavity of the active site. The binding of tropolone in this cavity is to some degree similar to that of PTU-catechol oxidase binding. The tropolone ring forms van der Waals interactions with the residues in the cavity. In this structure, the carboxyl oxygen of tropolone is positioned toward the binuclear copper center at a distance greater than required

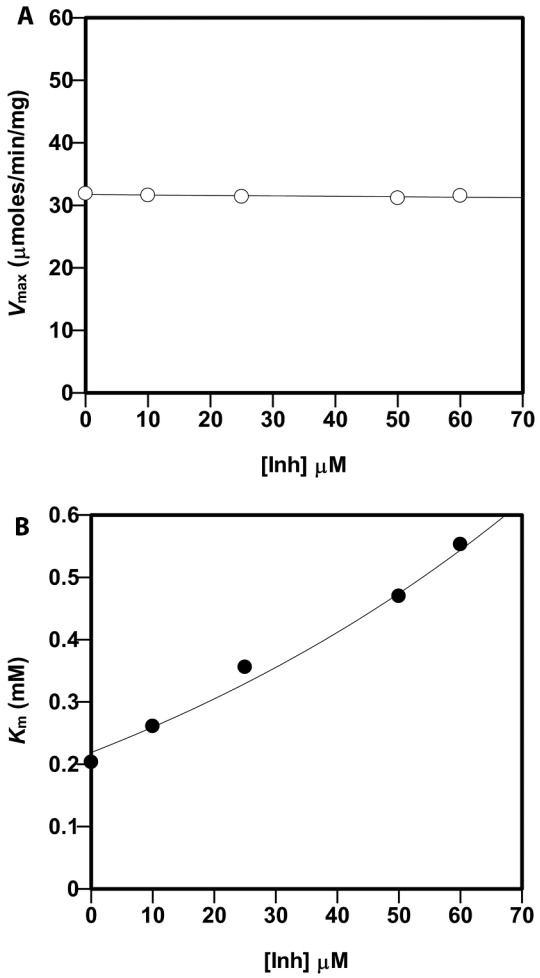

Fig. 1. Representative graphs depicting unchanged V_{max} value (A) with increasing substrate K_m (B) characteristic of competitive inhibition of tyrosinase by the target compounds.

for optimal interaction indicating that tropolone does not specifically bind to deoxytyrosinase [23]. However, previous studies on the crystal structure of tropolone binding to oxytyrosinase showed that it forms a pre-Michaelis complex in which it does interact with the Cu [30].

A more clear evidence of copper interaction comes from the crystal structure of PTU-catechol oxidase complex [24]. Inhibition of catechol oxidase by PTU requires coordination of the sulfur atom with the binuclear copper center and hydrophobic interactions with the large binding pocket of the active site. In this complex the sulfur atom of PTU replaces the hydroxo-bridge in the Cu(II)–Cu(II) center and coordinates with both copper ions. Additionally the amide nitrogen of the inhibitor weakly interacts with the CuB by forming a square-pyramidal coordination sphere (Fig. 4**A**).

Both of the crystal structures are promising for understanding the apparent binding mode of the target compounds to the tyrosinase active site. A mono-dentate binding mode is proposed for the carbazole and hydrazone derivatives. In the former, the terminal sulfur atom connecting the side groups is proposed to interact with the binuclear copper center by replacing the hydroxo-bridge in the Cu(II)–Cu(II) center (Fig. 4**B**). In the latter, the sulfur atom of the thiazole ring is proposed to replace the copper center bridge by interacting with it whereas the adjacent nitrogen atom of the hydrazone moiety is proposed to coordinate with the CuB of the center (Fig. 4**C**). Furthermore, role of the hydrophobicity of the compounds also counts; it apparently augments the inhibitor interactions with the binding pocket. The hydrazone derivatives are proposed to interact with the binuclear copper

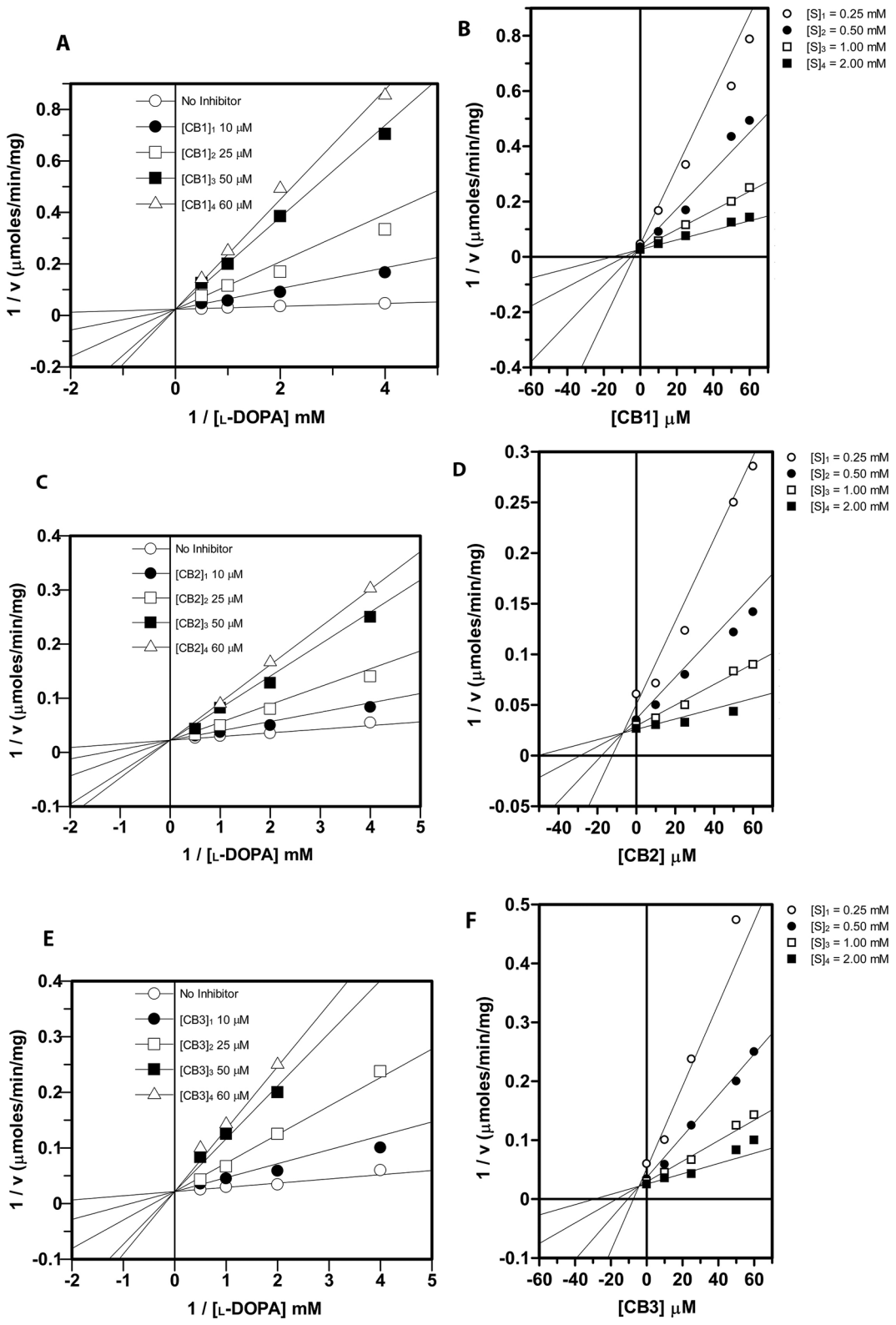

Fig. 2. Lineweaver-Burk (A, C, E) and Dixon plots (B, D, F) for representative carbazole inhibitors.

center through their thiazole ring sulfur atom. The exact binding conformation of the target carbazole and hydrazone derivatives is yet to be determined by X-ray crystallography, for which work is currently in progress.

Representative compounds from each of the carbazole (**CB1**, **CB7**) and hydrazone (**HZ1**) derivatives were subjected to copper binding studies to determine if they inhibited tyrosinase by specifically binding to the binuclear copper center of the active site. **CB1** (K_i = 1.64 μM) at 60 μM concentration, maximally inhibited the *o*-diphenolase activity of tyrosinase by showing a ΔA475 nm of 0.043/min. when compared to the control with no inhibitor (0.122/min.). Addition of $CuSO_4$ up to a maximum concentration of 0.35 mM caused the reversal of the *o*-

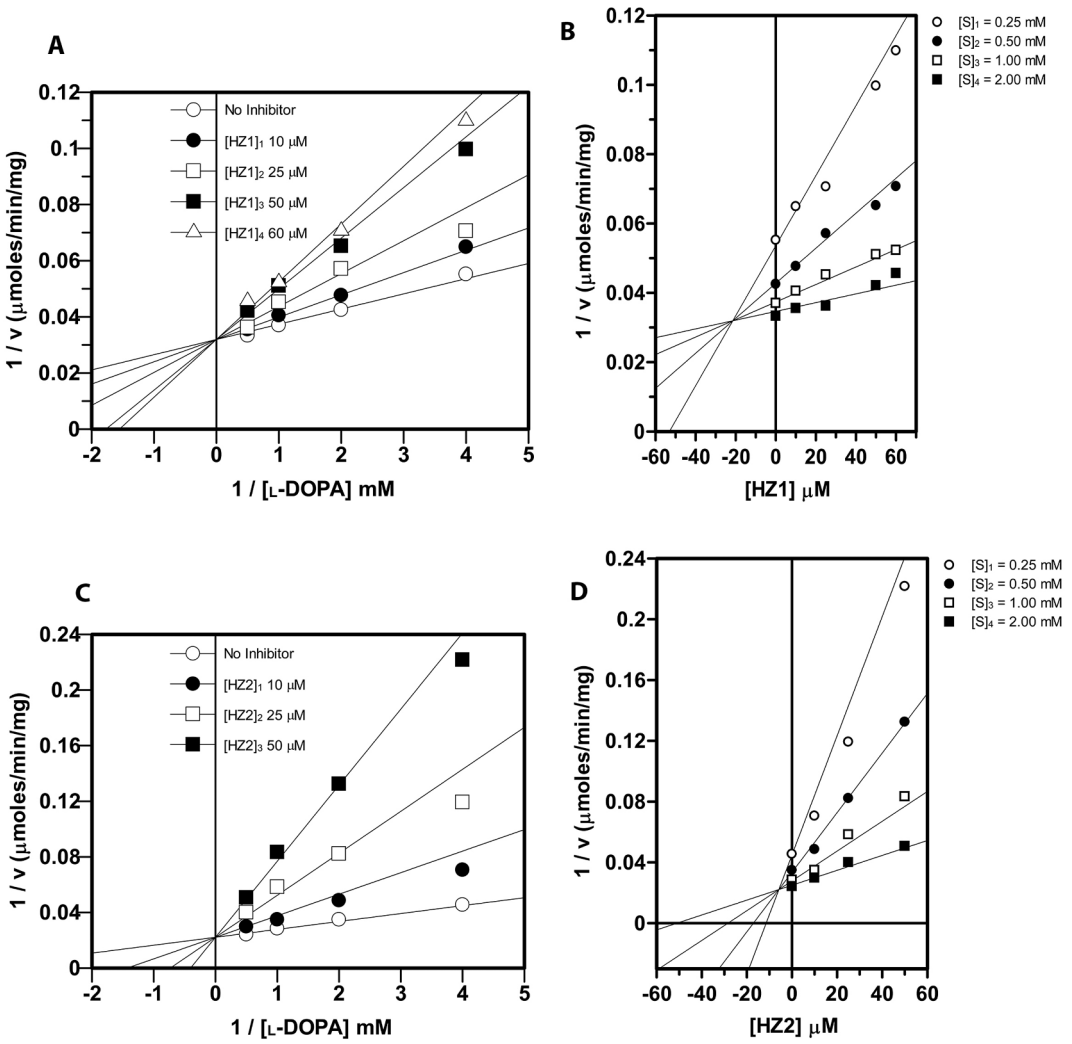

Fig. 3. Lineweaver-Burk (A, C) and Dixon plots (B, D) for representative hydrazone inhibitors.

diphenolase activity of tyrosinase by more than 35%. (Fig. 5**A**). No further recovery of the enzyme activity was observed beyond that concentration of $CuSO_4$ apparently due to high affinity of the inhibitor to the enzyme active site. In fact, the activity started to decline proportionally after 0.35 mM $CuSO_4$ indicating that $CuSO_4$ alone, exerted inhibitory effect on the unbound enzyme (Fig. 5**D**). Moreover, the activity reversal clearly indicated that the enzyme-inhibitor complex is reversible.

The activity recovery pattern of **CB7**-inhibited tyrosinase was similar to that of **CB1**, however, it is 5-fold less potent than the **CB1**. Therefore, in this case a lower concentration of $CuSO_4$ was needed for activity reversal. Addition of $CuSO_4$ up to a concentration of 0.05 mM was enough to reverse 63% of the *o*-diphenolase activity of **CB7**-inhibited tyrosinase (Fig. 5**B**).

Much lower concentration of $CuSO_4$ was needed to attain activity reversal of **HZ1**-inhibited tyrosinase because its affinity to tyrosinase was 13-fold and 3-fold lower than that of **CB1** and **CB7** respectively. Only 0.025 mM $CuSO_4$ was sufficient to recover approximately 89% of the enzyme activity (Fig. 5**C**). Therefore, a lower concentration of $CuSO_4$ was needed to displace it from the active site. These studies are

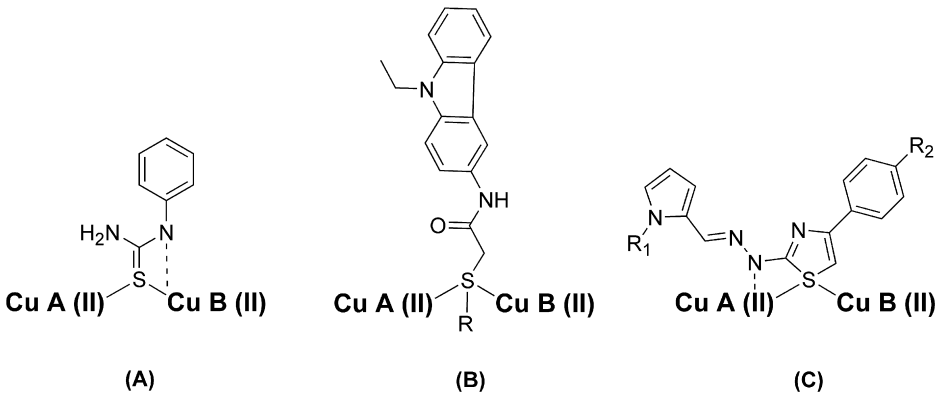

Fig. 4. (A). Interaction of PTU with the binuclear copper center of catechol oxidase as observed in the X-ray structure of the complex. Proposed binding of the carbazole (B) and hydrazone moieties (C) to the copper center of mushroom tyrosinase based on the experimental and structural evidence from the X-ray structures of catechol oxidase in complex with PTU and mushroom tyrosinase in complex with tropolone.

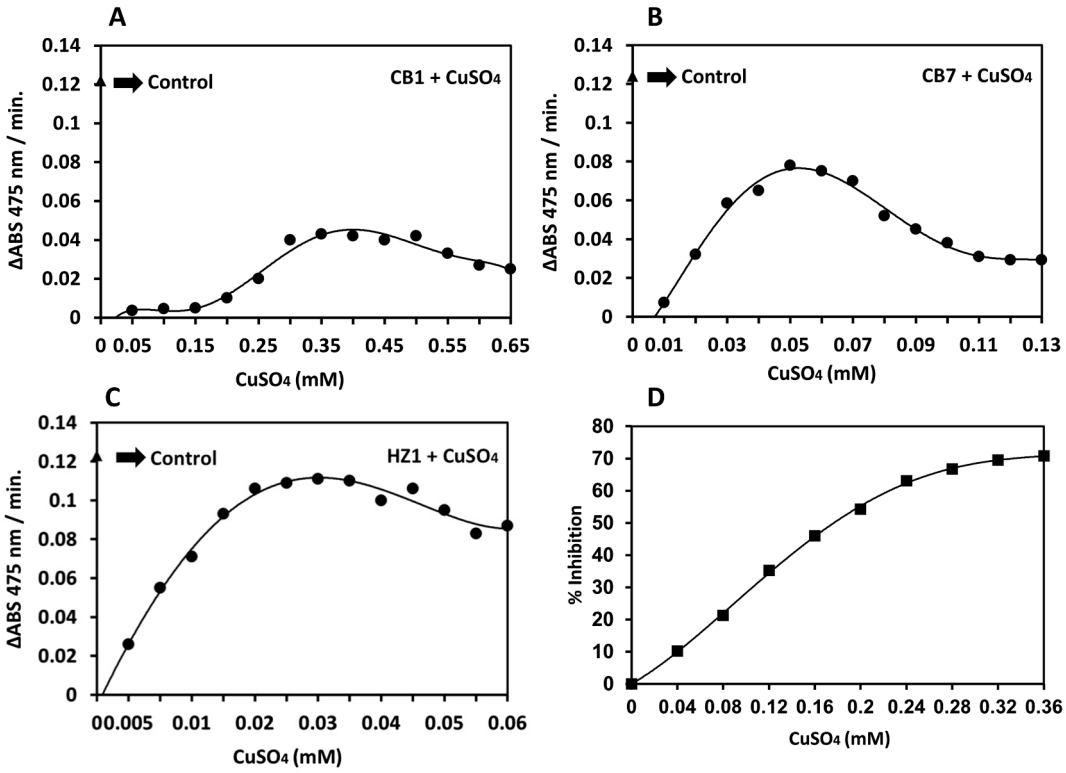

Fig. 5. Recovery of the *o*-diphenolase activity of tyrosinase pre-inhibited by (A) **CB1**, (B) **CB7** and (C) **HZ1**. (D). Effect of $CuSO_4$ alone on the tyrosinase activity.

convincing to conclude that the target compounds specifically interact with the binuclear copper center of the tyrosinase active site and it is unlikely that a mere copper chelation effect is responsible for their inhibitory activity.

3.4. Identification of active groups

3.4.1. Carbazole inhibitors

CB1 exhibited most potent inhibition of tyrosinase (K_i = 1.64 μM). Its 2-benzoimidazole substitution appears to be most conducive to tyrosinase inhibition. Other substitutions that were also favorable to enzyme inhibition included 2-(4,5-dihydrothiazole) in **CB4** (K_i = 3.46 μM) and 2-benzoxazole in **CB3** (K_i = 4.34 μM).

Among other carbazole derivatives, **CB2** with the 2-benzothiazole moiety also potently inhibited the enzyme (K_i = 6.87 μM). Similar potency of inhibition was also shown by **CB5**, **CB6** and **CB7** bearing the 2-(2-nitrophenoxy), 2-(3-ethylphenoxy) and 2-(3-chlorophenoxy) substitutions respectively. Apparently these substitutions in addition to the imidazole and thiazole rings with slight structural differences are favorable to tyrosinase active site binding that eventually exhibited comparable levels of inhibition. Interestingly, the 2-benzoimidazole ring in **CB1** was most favorable to enzyme inhibition that differed from the thiazole and oxazole rings only by a nitrogen atom.

3.4.2. Hydrazone inhibitors

The inhibitory activities of majority of the hydrazone derivatives were found to be comparable to each other with a K_i range of 4.95–21.45 μM. Since the structural differences within the members of this series of compounds is mainly contributed by the presence of the terminal groups, similarity in their K_i values clearly explains this phenomenon. **HZ4** (Ki = 4.95 μM) is slightly more potent than **HZ2** (Ki = 5.81 μM) as they are different from each other only by a chlorine atom. **HZ5**, bearing the 4-bromophenyl substitution also exhibited a level of inhibition similar to that of other members in the series.

Through these observations it is generally assumed that the enzyme is selective to the hydrazones containing halogens for tight binding except to fluorine. Different terminal groups present in these compounds mainly exhibited varying degree of tyrosinase inhibition. The order of potency was found to be in a narrow range as 4-chlorophenyl > 4-phenyl > 4-methoxy > 4-bromophenyl > 4-fluorophenyl. These substitutions made subtle differences between the levels of activities of the compounds indicating that the compounds apparently interact with the tyrosinase active site through a common binding mode.

4. Conclusions

Both carbazole and hydrazone derivatives showed potent and comparable levels of tyrosinase inhibition. The major active chemical groups in the carbazole derivatives beside the parent structure include the imidazole, thiazole and oxazole rings in addition to phenyl substitutions. As discussed earlier, this is in agreement with the fact that azole ring-containing compounds inhibit tyrosinase with varying degree of potencies. It is important to mention that the compound containing the imidazole ring exhibited highest level of tyrosinase inhibition.

The hydrazone derivatives also showed comparable levels of tyrosinase inhibition that appears to be mainly exerted by their terminal chemical groups. All these groups including the halogens potently inhibited tyrosinase except the one with a 4-fluorophenyl group that was found to be least favorable for enzyme inhibition.

The kinetic and copper binding studies on the representative compounds from both carbazole and hydrazone series showed that the compounds competitively bind to the tyrosinase active site by specifically interacting with its binuclear copper center.

Acknowledgement

The author would like to thank Prof. Dr. Asim Kaplancikli, Dr. Leyla Yurttaş, and their team from Department of Pharmaceutical Chemistry,

Faculty of Pharmacy, Anadolu University, Eskişehir, Turkey, for synthesizing the target compounds studied in the current work. The author would like to pay special gratitude to Prof. Dr. Fatih Demirci from Department of Pharmacognosy of the same university for facilitating synthesis of the compounds.

The author would also like to acknowledge the College of Medicine Research Center (CMRC) and the Deanship of Scientific Research at King Saud University, Riyadh, Saudi Arabia, for their support and funding this work.

Conflict of interest

The author has no conflict of interest.

Appendix A. Supplementary material

Supplementary data to this article can be found online at https://doi.org/10.1016/j.bioorg.2018.10.026.

References

[1] T. Pillaiyara, M. Manickamb, S.H. Jung, Recent development of signaling pathways inhibitors of melanogenesis, Cell. Signal. 40 (2007) 99–115.
[2] S.J. Ahn, et al., Regulation of melanin synthesis by selenium-containing carbohydrates, Chem. Pharm. Bull. 54 (2006) 281–286.
[3] K. Iozumi, G.E. Hoganson, R. Pennella, M.A. Everett, B.B. Fuller, Role of tyrosinase as the determinant of pigmentation in cultured human melanocytes, J. Invest. Dermatol. 100 (1993) 806–811.
[4] G. Li, H.K. Ju, H.W. Chang, Y. Jahng, S.H. Lee, J.K. Son, Melanin biosynthesis inhibitors from the bark of Machilus thunbergii, Biol. Pharm. Bull. 26 (2003) 1039–1041.
[5] N. Unver, et al., Alterations in the epidermal melanin axis and factor XIIIa melanophages in senile lentigo and ageing skin, Br. J. Dermatol. 155 (2006) 119–128.
[6] K. Urabe, J. Nakayama, Y. Hori, Mixed epidermal and dermal hypermelanoses, in: J.J. Norlund, J.R.E. Boissy, V.J. Hearing, R.A. King, W.S. Oetting, J.P. Ortonne (Eds.), The Pigmentary System: Physiology and Pathophysiology, Oxford University Press, New York, NY, USA, 1998, pp. 909–913.
[7] T. Pillaiyar, M. Manickam, V. Namasivayam, Skin whitening agents: medicinal chemistry perspective of tyrosinase inhibitors, J. Enz. Inh. Med. Chem. 32 (2017) 403–425.
[8] L.L. Shaoa, et al., Novel hydroxypyridinone derivatives containing an oxime ether moiety: synthesis, inhibition on mushroom tyrosinase and application in anti-browning of fresh-cut apples, Food Chem. 242 (2018) 174–181.
[9] S.H. Liu, I.H. Pan, I.M. Chu, Inhibitory effect of *p*-hydroxybenzyl alcohol on tyrosinase activity and melanogenesis, Biol. Pharm. Bull. 30 (2007) 1135–1139.
[10] Z.A. Kaplancikli, Synthesis of some novel Carbazole derivatives and evaluation of their antimicrobial activity, Marmara Pharmaceut. J. 15 (2011) 105–109.
[11] H.J. Knolker, W. Frohner, K.R. Reddy, Iron-mediated synthesis of carbazomycin G and carbazomycin H, the first carbazole-1,4-quinol alkaloids from *Streptoverticillium ehimense*, Eur. J. Org. Chem. 4 (2003) 740–746.
[12] H. Hagiwara, T. Choshi, H. Fujimoto, E. Sugino, S.A. Hibino, Novel total synthesis of antibiotic carbazole alkaloid carbazomycin G, Tetrahedron 56 (2000) 5807–5811.
[13] L. Yurttas, et al., Synthesis and antimicrobial activity of some new hydrazone-bridged thiazole-pyrrole derivatives, J. Enz. Inh. Med. Chem. 28 (2013) 830–835.
[14] U. Ghani, N. Ullah, New potent inhibitors of tyrosinase: Novel clues to binding of 1,3,4-thiadiazole-2(3H)-thiones, 1,3,4-oxadiazole-2(3H)-thiones, 4-amino-1,2,4-triazole-5(4H)-thiones, and substituted hydrazides to the binuclear active site, Bioorg. Med. Chem. 18 (2010) 4042–4048.
[15] V.D. Bock, D. Speijer, H. Hiemstraa, J.H. van Maarseveen, 1,2,3-Triazoles as peptide bond isosteres: synthesis and biological evaluation of cyclotetrapeptide mimics, Org. Biomol. Chem. 5 (2007) 971–975.
[16] F. Yu, et al., Synthesis of triazole schiff's base derivatives and their inhibitory kinetics on yyrosinase activity, PLoS One 10 (9) (2015) e0138578, 13 pages.
[17] W. Xie, et al., Synthesis and biological evaluation of kojic acid derivatives containing 1,2,4-triazole as potent tyrosinase inhibitors, Chem. Biol. Drug Des. 86 (2015) 1087–1092.
[18] M.M. El Sadek, et al., Synthesis and bioassay of a new class of furanyl-1,3,4-oxadiazole derivatives, Molecules 18 (2013) 8550–8562.
[19] K.W. Lam, et al., Synthesis and biological activity of oxadiazole and triazolothiadiazole derivatives as tyrosinase inhibitors, Bioorg. Med. Chem. Lett. 20 (2010) 3755–3759.
[20] M.T.H. Khan, et al., Structure–activity relationships of tyrosinase inhibitory combinatorial library of 2,5-disubstituted-1,3,4-oxadiazole analogues, Bioorg. Med. Chem. 13 (2005) 3385–3395.
[21] R.L. Sawant, P.D. Lanke, J.B. Wadekar, Tyrosinase inhibitory activity, 3D QSAR, and molecular docking study of 2,5-Disubstituted-1,3,4 Oxadiazoles, J. Chem. (2013) Article ID 849782, 7 pages.
[22] A.R. Nixha, et al., Synthesis and theoretical calculations of carbazole substituted chalcone urea derivatives and studies their polyphenol oxidase enzyme activity, J. Enz. Inh. Med. Chem. 28 (2013) 808–815.
[23] T. Klabunde, C. Eicken, J.C. Sacchettini, B. Krebs, Crystal structure of a plant catechol oxidase containing a dicopper center, Nat. Struct. Biol. 5 (1998) 1084–1090.
[24] W.T. Ismaya, H.J. Rozeboom, A. Weijn, J.J. Mes, F. Fusetti, H.J. Wichers, B.W. Dijkstra, Crystal structure of Agaricus bisporus mushroom tyrosinase: identity of the tetramer subunits and interaction with tropolone, Biochemistry 50 (2011) 5477–5486.
[25] Z.A. Kaplancikli, et al., Synthesis, antimicrobial activity and cytotoxicity of some new carbazole derivatives, J. Enz. Inh. Med. Chem. 27 (2012) 868–874.
[26] V.J. Hearing Jr., Mammalian monophenol monooxygenase (tyrosinase): purification, properties, and reactions catalyzed, Methods Enzymol. 142 (1987) 154–165.
[27] V. Kahn, A. Andrawis, Tropolone as a substrate for horseradish peroxidase, Phytochemistry 24 (1985) 905–913.
[28] H. Lineweaver, D. Burk, The determination of enzyme dissociation constants, J. Am. Chem. Soc. 56 (1934) 658–666.
[29] M. Dixon, The determination of enzyme inhibitor constants, Biochem. J. 55 (1953) 170–171.
[30] W.M. Macintyre, J.M. Robertson, R.F. Zahrobski, Crystal structure of cupric tropolone – a refinement, Proc. R. Soc. London A 289 (1966) 161–170.